Published in final edited form as:

Dev Cell. 2012 April 17; 22(4): 871–878. doi:10.1016/j.devcel.2012.01.020.

Snf2l Regulates Foxg1-Dependent Progenitor Cell Expansion in the Developing Brain

Darren J. Yip[1,3,6], **Chelsea P. Corcoran**[1,3,6], **Matías Alvarez-Saavedra**[1,4,6], **Adriana DeMaria**[1], **Stephen Rennick**[1,3], **Alan J. Mears**[2,4], **Michael A. Rudnicki**[1,4], **Claude Messier**[5], and **David J. Picketts**[1,3,*]

[1]Regenerative Medicine Program, Ottawa Hospital Research Institute, Ottawa, ON K1H 8L6, Canada

[2]Vision Program, Ottawa Hospital Research Institute, Ottawa, ON K1H 8L6, Canada

[3]Department of Biochemistry, Microbiology, and Immunology, University of Ottawa, Ottawa, ON K1H 8M5, Canada

[4]Department of Cellular and Molecular Medicine, University of Ottawa, Ottawa, ON K1H 8M5, Canada

[5]School of Psychology, University of Ottawa, Ottawa, ON K1H 8M5, Canada

SUMMARY

Balancing progenitor cell self-renewal and differentiation is essential for brain development and is regulated by the activity of chromatin remodeling complexes. Nevertheless, linking chromatin changes to specific pathways that control cortical histogenesis remains a challenge. Here we identify a genetic interaction between the chromatin remodeler Snf2l and Foxg1, a key regulator of neurogenesis. *Snf2l* mutant mice exhibit forebrain hypercellularity arising from increased *Foxg1* expression, increased progenitor cell expansion, and delayed differentiation. We demonstrate that Snf2l binds to the *Foxg1* locus at midneurogenesis and that the phenotype is rescued by reducing *Foxg1* dosage, thus revealing that Snf2l and Foxg1 function antagonistically to regulate brain size.

INTRODUCTION

The development of the mammalian forebrain is a tightly regulated process that involves expansion of the neural progenitor pool followed by waves of asymmetric division to generate an array of specialized neuronal subtypes that comprise the six layers of the cortex (Gupta et al., 2002). The decision of precursor cells to self renew or differentiate is regulated

*Correspondence: dpicketts@ohri.ca.

[6]These authors contributed equally to this work

ACCESSION NUMBERS

The microarray data are available in the Gene Expression Omnibus (GEO) database (http://www.ncbi.nlm.nih.gov/gds) under the accession number GSE34998.

SUPPLEMENTAL INFORMATION

Supplemental Information includes four figures and two tables and can be found with this article online at doi:10.1016/j.devcel.2012.01.020.

by extrinsic factors and a cell intrinsic program largely mediated by neurogenic transcription factors (Götz and Huttner, 2005; Guillemot, 2007; Shen et al., 2006). The role of epigenetic factors in forebrain development is implicit based in part, on the rising number of neurodevelopmental disorders caused by mutations in genes encoding chromatin remodeling proteins (van Bokhoven and Kramer, 2010). Further, the use of mouse models and neural stem cell cultures have begun to elucidate the epigenetic mechanisms controlling neurogenesis (Bérubéet al., 2005; Fasano et al., 2009; Lessard et al., 2007; Lim et al., 2009; Molofsky et al., 2005; Molofsky et al., 2003). Nonetheless, the continued deciphering of the interplay between epigenetic regulators and neurogenic transcription factors is paramount to our understanding of forebrain development.

The mammalian *ISWI* chromatin remodeling proteins, Snf2h and Snf2l, are components of multiple protein complexes with diverse functions that include nucleosome assembly/spacing during replication and transcriptional regulation (Dirscherl and Krebs, 2004). In the developing brain, *Snf2h* expression is prevalent in progenitor cells whereas *Snf2l* expression increases during terminal differentiation (Barak et al., 2003; Lazzaro and Picketts, 2001). Other studies suggest these genes may have distinct roles during neural development. Inactivation of *Snf2h* results in proliferation defects and embryonic lethality in mice whereas ectopic expression of *Snf2l* induces terminal differentiation of cultured neuroblastoma cells (Barak et al., 2003; Stopka and Skoultchi, 2003). To further assess the in vivo requirement for Snf2l we used a conditional targeting approach to impair remodeling activity by the removal of the ATP-binding motif of the *Snf2l* gene. These *Snf2l* mutant mice exhibit deregulated *Foxg1* expression resulting in enhanced progenitor expansion, delayed neurogenesis and hypercellularity in the murine brain.

RESULTS AND DISCUSSION

Hypercellularity in Snf2l-Deficient Mice

We utilized a conditional gene targeting approach by inserting loxP sites that flanked exon 6 (Figure 1A). Exon 6 encodes the ATP-binding motif of the SNF2 domain that is critical for the chromatin remodeling activity of Snf2l containing protein complexes (Figure 1A). To assess the impact of widespread early embryonic loss of *Snf2l* activity we bred $Snf2l^{f/f}$ mice to GATA1-Cre animals, which exhibit ubiquitous and early embryonic Cre activity (Mao et al., 1999). Unlike the embryonic lethality of *Snf2h* null mice (Stopka and Skoultchi, 2003), the $Snf2l^{f/Y}$; GATA1-$Cre^{+/-}$ animals were healthy, fertile, and born at normal Mendelian ratios. As such, we bred the exon 6-deleted allele independent of Cre recombinase (hereafter named Ex6DEL).

The Ex6DEL male mice expressed a stable *Snf2l* transcript lacking exon 6 and produced a corresponding protein product reduced in size by 7 kDa (Figures 1B and S1A available online). The mice displayed no overt phenotype and performed equally well to wild-type (WT) littermates in several behavior tests (Figures S1B–S1D). The only gross morphological difference we observed was that the Ex6DEL animals had larger heads (Figure S1E). Because Snf2l can promote neuronal differentiation in vitro, we reasoned that the loss of Snf2l activity might result in unfettered proliferation and increased brain size. Indeed, there was a 1.4-fold increase in the Ex6DEL brain:body mass ratio (Figure 1C) that

arose from an increased brain mass (0.65 g ± 0.18 g; n = 29; 8–43 weeks of age) compared to WT littermates (0.48 g ± 0.06 g; n = 26; $p = 1.53 \times 10^{-5}$), with no difference in body weight (Ex6DEL, 36.5 g ± 6.8 g; WT, 37.9 g ± 7.6 g; p = 0.48). Homozygous Ex6DEL female mice showed a similar increase in brain:body mass ratio, whereas heterozygous Ex6DEL females had normal ratios, suggesting that the Ex6DEL allele is not functioning as a dominant-negative or gain-of-function allele but is consistent with a loss-of-function phenotype (Figure 1C). A similar analysis of multiple organs at a single age (11 weeks) showed that heart mass was the only other organ increased in size (Table S1). We conclude that the Ex6DEL mice have an increase in organ mass that primarily affects the brain.

To characterize the brains we measured cortical thickness at medial and medial-lateral positions in both rostral and caudal sections of P7 brains. A statistically significant increase in thickness throughout the medial region of the Ex6DEL cortex was observed (Figures 1D and 1E and S1F). To determine if increased cortical thickness correlated with cell number we performed cell counts and observed hypercellularity within the cortex at several ages (Figures 1F–1H). Specifically, increased cell density was observed beginning embryonically at E15.5, although at this age statistical significance was restricted to the ventricular zone (VZ; Figure 1F). At P7, cell density was increased in cortical layers II/III (Ex6DEL 504 ± 16 cells; WT 440 ± 22 cells; n = 4; p = 0.015), IV (Ex6DEL 364 ± 30 cells; WT 238 ± 16 cells; n = 4; p = 0.003), and V/VI (Ex6DEL 423 ± 16 cells; WT 258 ± 30 cells; n = 4; p = 0.001) (Figure 1G). Similarly, the Ex6DEL adult cortex also showed increased cell density in the cortical layers (Figure 1H). We conclude that *Snf2l* loss causes hypercellularity and an increased brain mass without significantly altering the structural morphology of the cortex.

Increased Progenitor Self-Renewal in Developing Brain of Ex6DEL Mice Increased cell numbers can arise from decreased cell death, changes in cell cycle kinetics, or increased self-renewal. We did not observe any differences in the proportion of apoptotic cells by TUNEL staining in WT or mutant mice indicating that altered cell survival is not the cause of the hypercellularity (Figures S1G and S1H). As an initial measure of cell kinetics we stained for mitotic cells at E15.5 using antibodies to phospho-histone H3 (PH3). We observed a 2.9-fold increase in the proportion of mitotic cells in the VZ of Ex6DEL mice compared to control animals ($0.118 \pm 7.9 \times 10^{-5}$ versus 0.040 ± 0.002 per 125 μm^2, respectively; n = 3; $p < 0.05$) prompting us to investigate other cell cycle parameters (Figures 2A and 2B). Next, we examined the proportion of S-phase cells by pulse-labeling cells with 5-bromo-2′-deoxyuridine (BrdU) at E13.5, 15.5, and 17.5 (Figures 2C and 2D). We observed a statistically significant increase in $BrdU^+$ cells in the Ex6DEL neocortex at E13.5 (1.47-fold increase; n = 4; p = 0.0488) and at E15.5 (1.35-fold increase; n = 6; p = 0.0074). A similar trend, albeit not significant, was also observed at E17.5 (1.26-fold increase; n = 3; p = 0.1503). An increased proportion of cells in both S- and M-phase suggest that proliferation is increased in the Ex6DEL animals.

Consistent with increased proliferation, we observed increased numbers of proliferating apical ($Pax6^+/BrdU^+$) and intermediate/ basal ($Tbr2^+/BrdU^+$) progenitor cells (IPCs) in the Ex6DEL neocortex at E13.5 (Figures 2E and 2F and S2A). By E15.5, the level of proliferating apical progenitors was normal, whereas IPC numbers ($Tbr2^+$) remained increased (Figure 2F). As a more direct assessment of cell cycle kinetics we used Idu/BrdU

double labeling to measure S-phase length (Fukumitsu et al., 2006). We observed that S-phase length was significantly shorter in the Ex6DEL animals at E15.5 confirming that the progenitors cycled at a faster rate (Figure 2G). A similar trend was observed at E13.5, although significance was not attained.

To address the possibility that increased self-renewal also contributed to the increased number of proliferating progenitors, cells were pulse-labeled with BrdU at E12.5, or E16.5 and the brains harvested 1 day later for staining with Ki67 antigen, a protein expressed in all dividing cells. The number of $BrdU^+$ $Ki67^+$ double-labeled cells represents the proportion of progenitors that have remained in cycle. We observed a significant increase in the proportion of double-labeled cells in the mutant animals at E13.5 (WT: 39.2 ± 3.2%; Ex6DEL: 50.8 ± 4.2%; n = 9; p = 0.0056) suggesting that a greater fraction of progenitors undergo self-renewal within a 24 hr period (Figures 3A and 3B). A similar increase was observed in the mutants at E17.5 (Figure 3B). Taken together, the data demonstrate that increased hypercellularity observed in the Ex6DEL mice results from a combination of an increased progenitor cell cycle rate and enhanced self-renewal, primarily of IPCs.

Altered Timing of Neurogenesis and Increased Neuronal Output

The altered proliferation of Ex6DEL progenitors coupled with the increased cortical thickness prompted us to examine the forebrain for changes in cortical lamination, the timing of neurogenesis, and the production of both deep (layer V, VI) and superficial (layers II–IV) neurons. Staining with six different layer-specific markers at several stages (E15.5, 17.5, 18.5) revealed that each marker was expressed in its correct laminar position (see Figures 3C and 3E, S2B and S2E, and S3B and S3C). Marker positive cell counts at E18.5 revealed that both early-born deep (Nurr1, CTIP2) and later-born superficial (Satb2, Cux1) neurons were increased in number (Figures S2C and S3A and S3D). Nonetheless, this was not true of all markers (e.g., Foxp1) indicating that specific fate changes are likely occurring in the Ex6DEL mice. For example, alternate corticofugal neuronal identities within layer V/VI are characterized by CTIP2 and Tbr1 levels. We observed a qualitative increase in the proportion of $CTIP2^{high}/Tbr1^{low}$ expressing cells at E15.5 within layers V/VI (Figure S2E) that could be suggestive of a fate change (McKenna et al., 2011). Similarly, at E17.5 the number of $CTIP2^+$ cells in layer V remained high and we observed a reduction in $Foxp1^+$ cells (Figure S3B), which may be reflective of altered sensory motor projections (Sürmeli et al., 2011). Taken together, these observations highlight that the Ex6DEL phenotype is complex with specific fate changes likely accompanying the increased neuronal output within the cortical layers.

The cortical plate is established by the successive birth of neurons that migrate to different layers. Layer I neurons are born at ~E11.5 followed around E12.5 by the production of layer VI and layer V neurons, respectively. Thus, a delay in cell cycle exit would be predicted to result in a shift in the timing of this sequence such that the production of “early” neurons will occur at later stages. To examine whether additional progenitor cell division(s) altered the timing of neurogenesis we pulse-labeled progenitors with BrdU at E12.5 then double labeled cells at E18.5 for BrdU and CTIP2, a marker of layer V–VI neurons. Brightly fluorescent BrdU-labeled cells (BrdU staining >75% of nucleus) are representative of cells

born at E12.5. We observed a significant reduction in the number of CTIP2/BrdU-double positive cells in layer V of the mutant cortex (Figures 3C and 3D). Indeed, the majority of the brightly fluorescent cells in the Ex6DEL cortex resided within layers 1 and VI suggesting that the neurons "born" at E12.5 in the mutants were adopting fates that are characteristic of an earlier stage. Similar results were obtained for Nurr1 (Figure S2D). Thus, aberrant Snf2l function disrupts progenitor cell cycle kinetics, self-renewal decisions, and alters the timing of neurogenesis that collectively, increases overall cell number in the developing Ex6DEL neocortex.

Foxg1 Is Misregulated in Ex6DEL Mice

Gene profiling at E15.5 revealed a significant increase in the expression of *Foxg1* in the mutant cortex that was confirmed by qPCR (Table S2 and Figure 4A). *Foxg1*/*Brain factor-1* is a forkhead homeodomain transcription factor that controls NSC self-renewal, IPC expansion and the timing of neurogenesis (Fasano et al., 2009; Shen et al., 2006; Siegenthaler and Miller, 2005; Siegenthaler et al., 2008). Mice deficient in *Foxg1* have a severe reduction in the size of the cerebral hemispheres as neural progenitors undergo premature differentiation, exhaust the progenitor pool at the expense of late-born neurons, and undergo lateral to medial repatterning of Cajal-Retzius neurons (Dou et al., 1999; Hanashima et al., 2004; Muzio and Mallamaci, 2005; Xuan et al., 1995). Conversely, NSCs transduced with Foxg1-expressing lentiviral vectors increased the neural progenitor pool, delayed neurogenesis, and increased neuronal output (Brancaccio et al., 2010). Thus, we postulated that increased *Foxg1* expression represented an excellent mechanism to explain the Ex6DEL phenotype. Consistent with this hypothesis, *Foxg1* protein levels were increased in the mutant animals compared to WT mice (Figures 4B and S4A–S4C). Notably, the SVZ is comprised of a mixture of high and low *Foxg1* expressing cells and the expression persists at a high level in the cortical plate (Figures 4B and S4B and S4C).

Recent studies have shown that Foxg1 mediates the repression of *Cdkn1a* (p21Cip1) to inhibit cell cycle exit and promote IPC expansion (Siegenthaler and Miller, 2005; Siegenthaler et al., 2008). Consistent with the increase in Foxg1 we observed a reduction in the expression of *Cdkn1a* in the mutant brains (Figure 4A). We also assessed the expression of other cdk inhibitors and observed reduced expression of *Cdnk1b* (p27Kip1) and *Cdnk2a* (p16INK4a) but not *Cdnk1c* (p57Kip2). We conclude that the Ex6DEL mice have altered *Foxg1* expression that affects downstream target gene expression.

We reasoned that Snf2l complexes are recruited to the *Foxg1* locus to limit the expression level of the gene and promote terminal differentiation. To assess whether Snf2l is enriched at the *Foxg1* gene we performed chromatin immunoprecipitation (ChIP) assays. Chromatin isolated from cortices dissected from E15.5 embryos was incubated with a Snf2l antibody previously used to identify Snf2l target genes, or with sheep IgG as a negative control (Barak et al., 2003; Lazzaro et al., 2006). Eleven amplicons (R1–R11) were designed for qPCR that span the *Foxg1* gene (Figure 4C). The results of these experiments (Figure 4D) showed that Snf2l binding was specifically enriched at the region that encompasses the P1 promoter (R8, $p \leq 0.012$), which drives expression of the more abundant class 1 *Foxg1* transcript (Li et al., 1996). Luciferase reporter assays confirmed the importance of a 1.2 kb

fragment for gene expression. Although this fragment encompassed the R8 region, addition of Snf2l or Snf2h in the assay system did not have any effect indicating that the functionality may be context-dependent (Figures S4D–S4F). Nonetheless, we conclude that Snf2l binds to the *Foxg1* gene, consistent with a direct role for Snf2l-containing complexes in the regulation of *Foxg1* expression. These results further suggest that misregulation of *Foxg1* underlies the phenotype of Ex6DEL mice.

Reduction of Foxg1 Rescues the Ex6DEL Phenotype

If Snf2l-containing chromatin remodeling complexes are required to regulate *Foxg1* expression then we predicted that genetic reduction of *Foxg1* dosage should rescue the phenotype of the Ex6DEL mice. Ex6DEL mice were bred to *Foxg1* heterozygous mice and the resulting Ex6DEL; Foxg1$^{+/-}$ animals were examined at E15.5 for signs of genetic rescue. In this regard, we examined the proportion of mitotic cells and the fraction of IPCs. As shown in Figures 4E and S4G, WT and *Foxg1* heterozygous mice had no significant difference in the proportion of PH3^{+} cells (0.034 ± 0.003 versus 0.033 ± 0.004 per fixed area). The Ex6DEL mice had a 3-fold increase in PH3^{+} cells (0.107± 0.006) but this was rescued in the Ex6DEL; Foxg1$^{+/-}$ animals (0.039 ± 0.002). Similarly, only the Ex6DEL mice showed a significant difference in the percentage of Tbr2/BrdU-double-positive cells in the VZ/SVZ of E15.5 cortical sections when compared to WT or *Foxg1* heterozygous littermates (Figures 4F and 4G). Remarkably, the increase in double positive cells was completely rescued when *Foxg1* dosage was reduced demonstrating that the increased IPC numbers was dependent on *Foxg1* expression levels (Figures 4F and 4G). Taken together, these data demonstrate that Snf2l functions in the same genetic pathway as Foxg1 to control the balance between progenitor proliferation and differentiation.

Modification of chromatin structure has emerged as a fundamental process controlling brain development through disease gene identification and a growing number of in vitro studies examining NSC proliferation and differentiation (Hamby et al., 2008; van Bokhoven and Kramer, 2010). In this study, we identify a genetic link between Foxg1 and the chromatin remodeling protein Snf2l that is important for regulating the balance between progenitor self-renewal and differentiation. We predict that Snf2l remodeling at the *Foxg1* gene results in its transcriptional repression and the subsequent de-repression of p21, thereby promoting the timely exit and terminal neuronal differentiation of progenitors that ultimately, controls brain size (Figure 4H). Studies in *Drosophila* and yeast demonstrate a well-documented role for ISWI in transcriptional repression often in association with the Sin3 repressive complex (Burgio et al., 2008; Fazzio et al., 2001). Other studies highlight a more global role for ISWI in chromatin compaction (Corona et al., 2007; Li et al., 2010). The Snf2l protein is part of two different complexes, CERF (Banting et al., 2005) and NURF (Barak et al., 2003), but which one regulates Foxg1 expression is unclear. The NURF complex is largely considered an activator of gene expression, whereas the function of the CERF complex remains unknown (Lazzaro et al., 2006; Wysocka et al., 2006). Because the Ex6DEL cortical phenotype is mild, the possibility exists that Snf2h-containing or other chromatin remodeling complexes may be providing some compensation. Indeed, future studies are required to delineate the specific roles of the ISWI-containing complexes in neural progenitor regulation. Nonetheless, an increased cortical cell density is most likely

compensated by a reduction in another component of the tissue (e.g., elaboration of neuronal projections). Additional studies will be required to define such changes although they may be related to corticofugal and sensory-motor projections as reflected by altered CTIP2- and Foxp1-positive cell numbers in the Ex6DEL animals.

EXPERIMENTAL PROCEDURES

Generation and Maintenance of Ex6DEL Mice

A 4.84 kb KpnI/*Xmn*I genomic fragment encompassing exon 6 of the m*Snf2l* gene was used to generate the targeting vector. A single loxP site was introduced distal to exon 6 (Pst1-EcoR1) and a Neo cassette flanked by loxP sites was inserted proximally (Xba1-Pst1) leaving short and long homologous arms of 1.6 kb and 2.6 kb, respectively. The targeting construct was electroporated into J1 ES cells, and G418-resistant clones were selected as described previously (Li et al., 1992). Homologous recombinants identified by Southern blot with probes located within exon 2 and exon 6, were utilized for blastocyst injection to generate exon 6 floxed mice. The exon 6 floxed line was bred to Gata1-Cre mice (Mao et al., 1999) to generate the Ex6DEL allele that was then maintained (independent of Cre) on a 129Sv background. Ex6DEL;Foxg1$^{+/-}$ mice were generated by crossing Ex6DEL mice to Foxg1-Cre knock-in animals (Hébert and McConnell, 2000). For timed mating purposes, the day of vaginal plug detection was counted as embryonic day 0.5 (E0.5). All experiments were approved by the University of Ottawa's Animal Care ethics committee adhering to the guidelines of the Canadian Council on Animal Care.

BrdU Labeling Experiments

Bromodeoxyuridine (BrdU) was administered by intraperitoneal injections (0.1 mg/g body weight) to time-mated females. For pulse labeling, pups were harvested 2 hr after a single injection. The percentage of BrdU$^+$ cells to total VZ cells were counted and normalized to WT levels for all embryonic time points. For cell cycle re-entry experiments, embryos pulse-labeled with BrdU at E12.5 or E16.5 were harvested 1 day later and stained for BrdU and the cell cycle marker Ki67. Cell cycle re-entry was determined as the proportion of cells that were BrdU$^+$ and Ki67$^+$ to the total number of BrdU$^+$ cells. For neuronal birthdating experiments, BrdU was injected at E12.5 and offspring harvested at E18.5 for processing. BrdU$^+$ cells were scored as densely labeled if BrdU comprised >75% of the nucleus. To determine S-phase length, iododeoxyuridine (IdU; 300 μg) was injected intraperitoneally into pregnant mares at gestational days E13.5 and 15.5. This was followed, 1.5 hr (T_i) later, by a similar injection of BrdU (300 μg). The female was euthanized and the embryos removed 30 min after the second injection. These two separate analogs were differentially detected by mouse anti-BrdU/IdU (1:100; BD Biosciences) and rat anti-BrdU/CldU (1:200; Abcam) antibodies. Cells positive for IdU but not BrdU have exited S phase (L_c) but double-labeled cells remain in S phase (S_c). Length of S phase was calculated as: $T_s = T_i \times S_c/L_c$ as described elsewhere (Martynoga et al., 2005).

Immunofluorescent Detection

Coronal brain sections (10 μm) were mounted on SuperFrost Slides (Fisher Scientific, ON) and frozen at −80°C until use. Sections were washed five times in PBST (PBS with 0.1%

Triton X-100), blocked (1 hr, room temperature) in 10% horse serum/PBST, and incubated (overnight, 4°C) in primary antibodies. The following primary antibodies were used: rat anti-BrdU (1:400); mouse anti-SATB2 (1:10); rat anti-CTIP2 (1:500); rabbit anti-FoxP1 (1:400); rabbit anti-Ki67 (1:250; NCL-Ki67-P, Novocastro); rabbit anti-Phosphohistone H3 antibody (1:100; 06–570, Upstate); rabbit anti-TBR2 (1:250; ab23345, AbCam); rabbit anti-Nurr1 (1:500, Santa Cruz, CA); mouse anti-β III tubulin (Tuj; 1:400 dilution; 01409, Stem Cell Technologies); and mouse anti-NeuN (1:500; Millipore). The following day, sections were washed five times in PBST and incubated (2 hr, RT) with DyLight^{488}, DyLight^{594}, or DyLight^{649}-conjugated secondary antibodies (1:1,000, Jackson ImmunoResearch, PA). All sections were counterstained with the nuclear marker DAPI (Invitrogen). Coverslips were mounted with Dako Fluorescence Mounting Medium (Dako Canada, ON).

Image Acquisition and Processing

For IF experiments, tissue sections were examined and images captured using a Zeiss 510 laser scanning confocal microscope with UV (405 nm), argon (488 nm), helium/neon (546 nm), and helium/neon (633 nm) lasers. All images were acquired as 8 μmZ stacks (in 2-μmintervals) and analyzed as projections using the LSM 510 Image Browser software (Zeiss). For cell density analysis, a 40-μm section was used to acquire 24 μm Z stacks (in 2-μm intervals) that were used for 3D reconstruction and cell counts. For counting of marker^{+} cells, we first determined the mean pixel intensity values using digital × axis and y axis pixel ovals placed within cortical brain regions or single cortical neurons (n > 50). Adigital oval (Φ100 pixels) was placed in immunoreactive negative brain regions and in adjacent “no primary” controls and the mean value was subtracted from the tissue under examination, thus generating a normalized immunoreactive positive intensity value that was used as the baseline to score a positive cell.

Chromatin Immunoprecipitation

The ChIP assay was performed as described in the protocol from the Millipore ChIP Assay Kit (product 17–295) with some modifications. Cerebral cortex was dissected from E15.5 Snf2l$^{f/f}$ mice. The tissue was mechanically dissociated and crosslinked in 1% paraformaldehyde for 1 hr on ice. Tissue from approx. 10 embryos (4×10^7 cells) was used for each experiment. Cells were lysed (50 mM Tris, 1 mM EDTA, 1% SDS, Roche Complete Mini protease inhibitor cocktail) on ice and then sonicated to generate fragments of 200–500 bp in length. Sepharose G slurry (25 μL; GE Biosciences) with 1 μg of either Sheep anti-Snf2l or Sheep IgG (Sigma) was used for IP. Quantitative PCR analysis was run on a MX3000P instrument (Stratagene) using Absolute QPCR SYBR Green Mix (Thermo Scientific). The cycling conditions were: one cycle at 95°C for 10 min and 40 cycles of 95°C for 30 s, 60°C for 30 s, 72°C for 30 s. Percent input of target DNA in the IP samples was calculated off a curve derived from serial dilutions of input chromatin.

Statistical Methods

For all data sets a minimum of three biological replicates (mice, embryos, or brains) were analyzed (n = 3). For cell counts, the mean cell number was determined from a minimum of three sections from three biological replicates and, in most instances the data was normalized to WT. Unless indicated otherwise, histograms represent the mean ± the

standard error of the mean (SEM). An asterisk (*) represents a statistically significant change by a two-tailed Student t test ($p \leq 0.05$) as compared to the WT sample, unless indicated differently by the use of brackets.

Supplementary Material

Refer to Web version on PubMed Central for supplementary material.

ACKNOWLEDGMENTS

We would like to thank K. Yan and J. Coulombe for technical assistance and Drs. R. Kothary, L. Megeney, and V. Wallace for helpful discussions and comments on the manuscript. The HSFCSR provided partial financial support toward the purchase of the confocal microscope used in this study. D.J.Y. was funded by an OGSST award. C.P.C. was an Ontario Graduate Scholarship recipient. D.J.P. was funded by CIHR operating grants.

REFERENCES

Banting GS, Barak O, Ames TM, Burnham AC, Kardel MD, Cooch NS, Davidson CE, Godbout R, McDermid HE, Shiekhattar R. CECR2, a protein involved in neurulation, forms a novel chromatin remodeling complex with SNF2L. Hum. Mol. Genet. 2005; 14:513–524. [PubMed: 15640247]

Barak O, Lazzaro MA, Lane WS, Speicher DW, Picketts DJ, Shiekhattar R. Isolation of human NURF: a regulator of Engrailed gene expression. EMBO J. 2003; 22:6089–6100. [PubMed: 14609955]

Bérubé NG, Mangelsdorf M, Jagla M, Vanderluit J, Garrick D, Gibbons RJ, Higgs DR, Slack RS, Picketts DJ. The chromatin-remodeling protein ATRX is critical for neuronal survival during corticogenesis. J. Clin. Invest. 2005; 115:258–267. [PubMed: 15668733]

Brancaccio M, Pivetta C, Granzotto M, Filippis C, Mallamaci A. Emx2 and Foxg1 inhibit gliogenesis and promote neuronogenesis. Stem Cells. 2010; 28:1206–1218. [PubMed: 20506244]

Burgio G, La Rocca G, Sala A, Arancio W, Di Gesù D, Collesano M, Sperling AS, Armstrong JA, van Heeringen SJ, Logie C, et al. Genetic identification of a network of factors that functionally interact with the nucleosome remodeling ATPase ISWI. PLoS Genet. 2008; 4:e1000089. [PubMed: 18535655]

Corona DF, Siriaco G, Armstrong JA, Snarskaya N, McClymont SA, Scott MP, Tamkun JW. ISWI regulates higher-order chromatin structure and histone H1 assembly in vivo. PLoS Biol. 2007; 5:e232. [PubMed: 17760505]

Dirscherl SS, Krebs JE. Functional diversity of ISWI complexes. Biochem. Cell Biol. 2004; 82:482–489. [PubMed: 15284901]

Dou CL, Li S, Lai E. Dual role of brain factor-1 in regulating growth and patterning of the cerebral hemispheres. Cereb. Cortex. 1999; 9:543–550. [PubMed: 10498272]

Fasano CA, Phoenix TN, Kokovay E, Lowry N, Elkabetz Y, Dimos JT, Lemischka IR, Studer L, Temple S. Bmi-1 cooperates with Foxg1 to maintain neural stem cell self-renewal in the forebrain. Genes Dev. 2009; 23:561–574. [PubMed: 19270157]

Fazzio TG, Kooperberg C, Goldmark JP, Neal C, Basom R, Delrow J, Tsukiyama T. Widespread collaboration of Isw2 and Sin3-Rpd3 chromatin remodeling complexes in transcriptional repression. Mol. Cell. Biol. 2001; 21:6450–6460. [PubMed: 11533234]

Fukumitsu H, Ohtsuka M, Murai R, Nakamura H, Itoh K, Furukawa S. Brain-derived neurotrophic factor participates in determination of neuronal laminar fate in the developing mouse cerebral cortex. J. Neurosci. 2006; 26:13218–13230. [PubMed: 17182772]

Götz M, Huttner WB. The cell biology of neurogenesis. Nat. Rev. Mol. Cell Biol. 2005; 6:777–788. [PubMed: 16314867]

Guillemot F. Spatial and temporal specification of neural fates by transcription factor codes. Development. 2007; 134:3771–3780. [PubMed: 17898002]

Gupta A, Tsai LH, Wynshaw-Boris A. Life is a journey: a genetic look at neocortical development. Nat. Rev. Genet. 2002; 3:342–355. [PubMed: 11988760]

Hamby ME, Coskun V, Sun YE. Transcriptional regulation of neuronal differentiation: the epigenetic layer of complexity. Biochim. Biophys. Acta. 2008; 1779:432–437. [PubMed: 18674649]

Hanashima C, Li SC, Shen L, Lai E, Fishell G. Foxg1 suppresses early cortical cell fate. Science. 2004; 303:56–59. [PubMed: 14704420]

Hébert JM, McConnell SK. Targeting of cre to the Foxg1 (BF-1) locus mediates loxP recombination in the telencephalon and other developing head structures. Dev. Biol. 2000; 222:296–306. [PubMed: 10837119]

Lazzaro MA, Pépin D, Pescador N, Murphy BD, Vanderhyden BC, Picketts DJ. The imitation switch protein SNF2L regulates steroidogenic acute regulatory protein expression during terminal differentiation of ovarian granulosa cells. Mol. Endocrinol. 2006; 20:2406–2417. [PubMed: 16740656]

Lazzaro MA, Picketts DJ. Cloning and characterization of the murine Imitation Switch (ISWI) genes: differential expression patterns suggest distinct developmental roles for Snf2h and Snf2l. J. Neurochem. 2001; 77:1145–1156. [PubMed: 11359880]

Lessard J, Wu JI, Ranish JA, Wan M, Winslow MM, Staahl BT, Wu H, Aebersold R, Graef IA, Crabtree GR. An essential switch in subunit composition of a chromatin remodeling complex during neural development. Neuron. 2007; 55:201–215. [PubMed: 17640523]

L E, Bestor TH, Jaenisch R. Targeted mutation of the DNA methyltransferase gene results in embryonic lethality. Cell. 1992; 69:915–926. [PubMed: 1606615]

Li H, Tao W, Lai E. Characterization of the structure and function of the gene for transcription factor BF-1, an essential regulator of forebrain development. Brain Res. Mol. Brain Res. 1996; 37:96–104. [PubMed: 8738140]

Li M, Belozerov VE, Cai HN. Modulation of chromatin boundary activities by nucleosome-remodeling activities in Drosophila melanogaster. Mol. Cell. Biol. 2010; 30:1067–1076. [PubMed: 19995906]

Lim DA, Huang YC, Swigut T, Mirick AL, Garcia-Verdugo JM, Wysocka J, Ernst P, Alvarez-Buylla A. Chromatin remodelling factor Mll1 is essential for neurogenesis from postnatal neural stem cells. Nature. 2009; 458:529–533. [PubMed: 19212323]

Mao X, Fujiwara Y, Orkin SH. Improved reporter strain for monitoring Cre recombinase-mediated DNA excisions in mice. Proc. Natl. Acad. Sci. USA. 1999; 96:5037–5042. [PubMed: 10220414]

Martynoga B, Morrison H, Price DJ, Mason JO. Foxg1 is required for specification of ventral telencephalon and region-specific regulation of dorsal telencephalic precursor proliferation and apoptosis. Dev. Biol. 2005; 283:113–127. [PubMed: 15893304]

McKenna WL, Betancourt J, Larkin KA, Abrams B, Guo C, Rubenstein JL, Chen B. Tbr1 and Fezf2 regulate alternate corticofugal neuronal identities during neocortical development. J. Neurosci. 2011; 31:549–564. [PubMed: 21228164]

Molofsky AV, He S, Bydon M, Morrison SJ, Pardal R. Bmi-1 promotes neural stem cell self-renewal and neural development but not mouse growth and survival by repressing the p16Ink4a and p19Arf senescence pathways. Genes Dev. 2005; 19:1432–1437. [PubMed: 15964994]

Molofsky AV, Pardal R, Iwashita T, Park IK, Clarke MF, Morrison SJ. Bmi-1 dependence distinguishes neural stem cell self-renewal from progenitor proliferation. Nature. 2003; 425:962–967. [PubMed: 14574365]

Muzio L, Mallamaci A. Foxg1 confines Cajal-Retzius neurono-genesis and hippocampal morphogenesis to the dorsomedial pallium. J. Neurosci. 2005; 25:4435–4441. [PubMed: 15858069]

Shen Q, Wang Y, Dimos JT, Fasano CA, Phoenix TN, Lemischka IR, Ivanova NB, Stifani S, Morrisey EE, Temple S. The timing of cortical neurogenesis is encoded within lineages of individual progenitor cells. Nat. Neurosci. 2006; 9:743–751. [PubMed: 16680166]

Siegenthaler JA, Miller MW. Transforming growth factor beta 1 promotes cell cycle exit through the cyclin-dependent kinase inhibitor p21 in the developing cerebral cortex. J. Neurosci. 2005; 25:8627–8636. [PubMed: 16177030]

Siegenthaler JA, Tremper-Wells BA, Miller MW. Foxg1 haploinsufficiency reduces the population of cortical intermediate progenitor cells: effect of increased p21 expression. Cereb. Cortex. 2008; 18:1865–1875. [PubMed: 18065723]

Stopka T, Skoultchi AI. The ISWI ATPase Snf2h is required for early mouse development. Proc. Natl. Acad. Sci. USA. 2003; 100:14097–14102. [PubMed: 14617767]

Sürmeli G, Akay T, Ippolito GC, Tucker PW, Jessell TM. Patterns of spinal sensory-motor connectivity prescribed by a dorsoventral positional template. Cell. 2011; 147:653–665. [PubMed: 22036571]

van Bokhoven H, Kramer JM. Disruption of the epigenetic code: an emerging mechanism in mental retardation. Neurobiol. Dis. 2010; 39:3–12. [PubMed: 20304068]

Wysocka J, Swigut T, Xiao H, Milne TA, Kwon SY, Landry J, Kauer M, Tackett AJ, Chait BT, Badenhorst P, et al. A PHD finger of NURF couples histone H3 lysine 4 trimethylation with chromatin remodelling. Nature. 2006; 442:86–90. [PubMed: 16728976]

Xuan S, Baptista CA, Balas G, Tao W, Soares VC, Lai E. Winged helix transcription factor BF-1 is essential for the development of the cerebral hemispheres. Neuron. 1995; 14:1141–1152. [PubMed: 7605629]

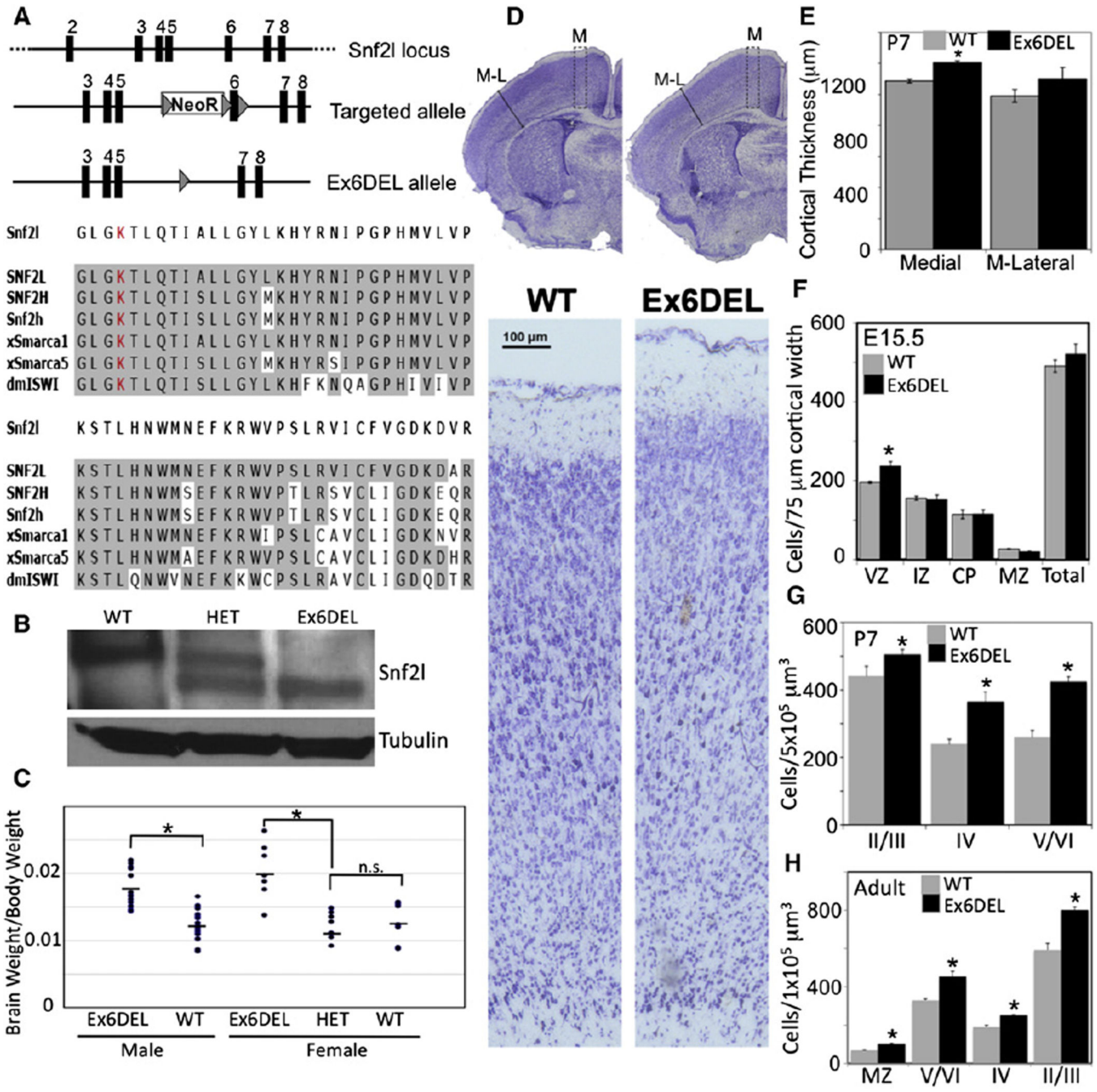

Figure 1. Increased Brain Mass and Cell Density in Ex6DEL Mice

(A) Schematic of the Snf2l locus, targeted allele, and the Ex6DEL allele (LoxP sites, gray triangles; NeoR, neomycin resistance gene). Below, sequence conservation of the 60 amino acids encoded by exon 6. Lys residue critical for ATPase activity is highlighted in red.

(B) Snf2l immunoblot of E15.5 cortical extracts from WT, HET, and Ex6DEL mice.

(C) Plot of brain weight to body weight ratios for Ex6DEL, WT, or HET mice. Brains from individual mice are represented by a dot with the mean indicated by a horizontal line.

(D and E) Nissl stained P7 rostral coronal brain sections (D) with high magnification images underneath (boxed areas in D) and corresponding plot (E) of cortical thickness from medial and medial-lateral regions.

(F) Cell counts from E15.5 cortical sections.

(G and H) Cell counts within a fixed brain volume from P7 (G) or Adult (H) brains. CP, cortical plate; II/III, IV, V/VI: cortical layers II and III, IV, and V and VI, respectively; IZ, intermediate zone; MZ, medial zone; n.s., not significant; VZ, ventricular zone. For (E–H), n = 4. Bars correspond to the mean values, whereas error bars indicate the SEM; an asterisk (*) represents a statistically significant change by a two-tailed paired Student t test ($p \leq 0.05$) as compared to the WT sample unless otherwise indicated by brackets.

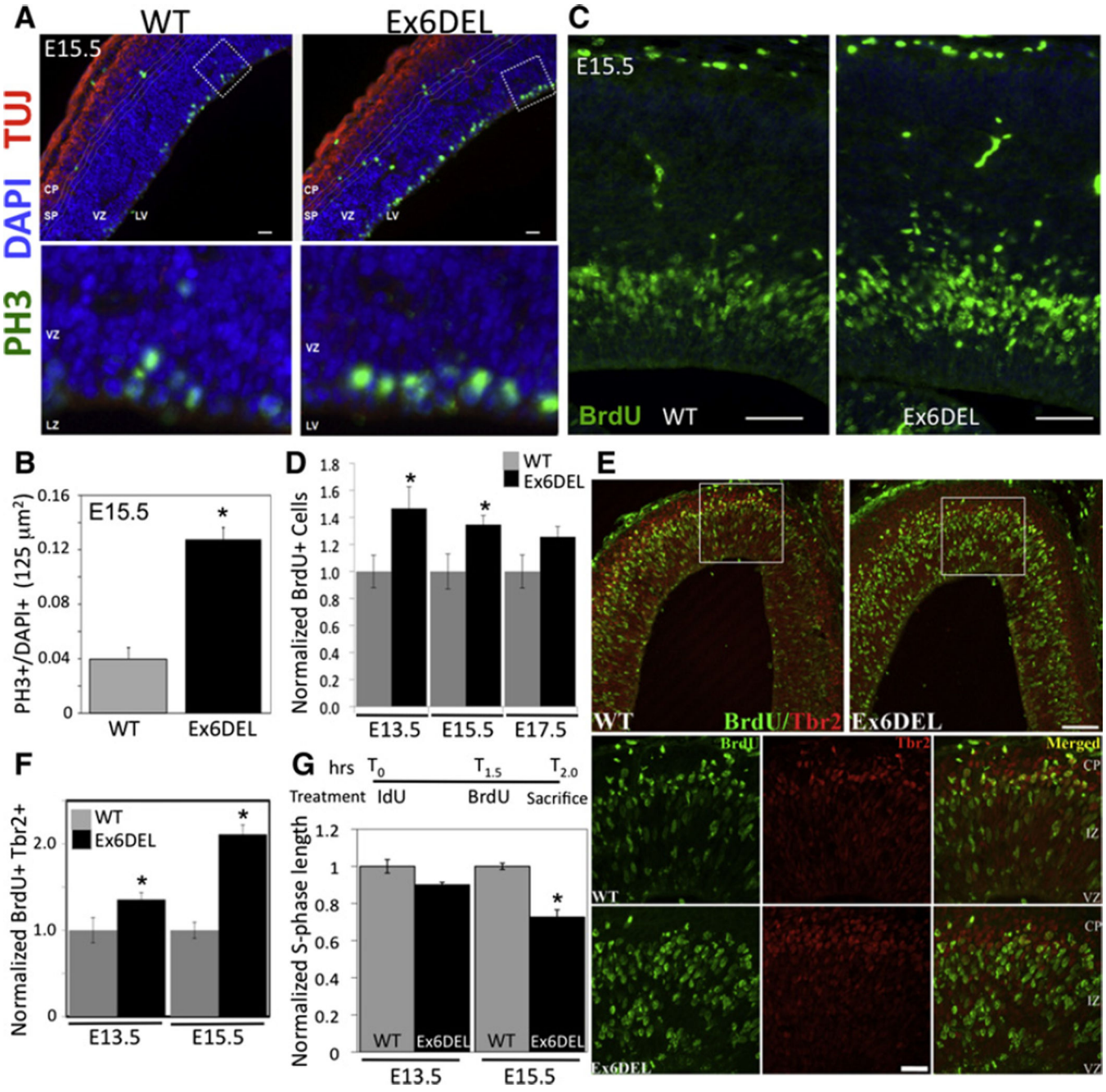

Figure 2. Ex6DEL Forebrains Have Altered Cell-Cycle Kinetics

(A) E15.5 forebrain sections stained for terminally differentiated neurons (Tuj) and mitotic progenitors (PH3). All nuclei are counterstained with DAPI. Boxed regions are enlarged below. Scale bar represents 30 μm.

(B) Quantification of $PH3^+$ cells to total cells in the VZ of E15.5 embryos (n = 3).

(C) E15.5 cortical sections stained for BrdU after a 2 hr pulse (n = 4). Scale bar represents 100 μm.

(D) Normalized plot of the percentage of $BrdU^+$ cells following a 2 hr BrdU pulse (n = 3).

(E and F) Tbr2 and BrdU double labeled E13.5 sections. Scale bar represents 100 μm. The boxed regions are shown below at higher magnification (scale bar represents 50 μm) and were representative of the images used to count the percentage of double-labeled cells (n = 3) shown in (F).

(G) Schematic of IdU and BrdU injection times to determine S-phase length. Plot of normalized S-phase length (h) at E13.5 and E15.5 (n = 3). For (B), (D), (F), and (G), bars represent the mean ± SEM; *$p < 0.05$ by t test.

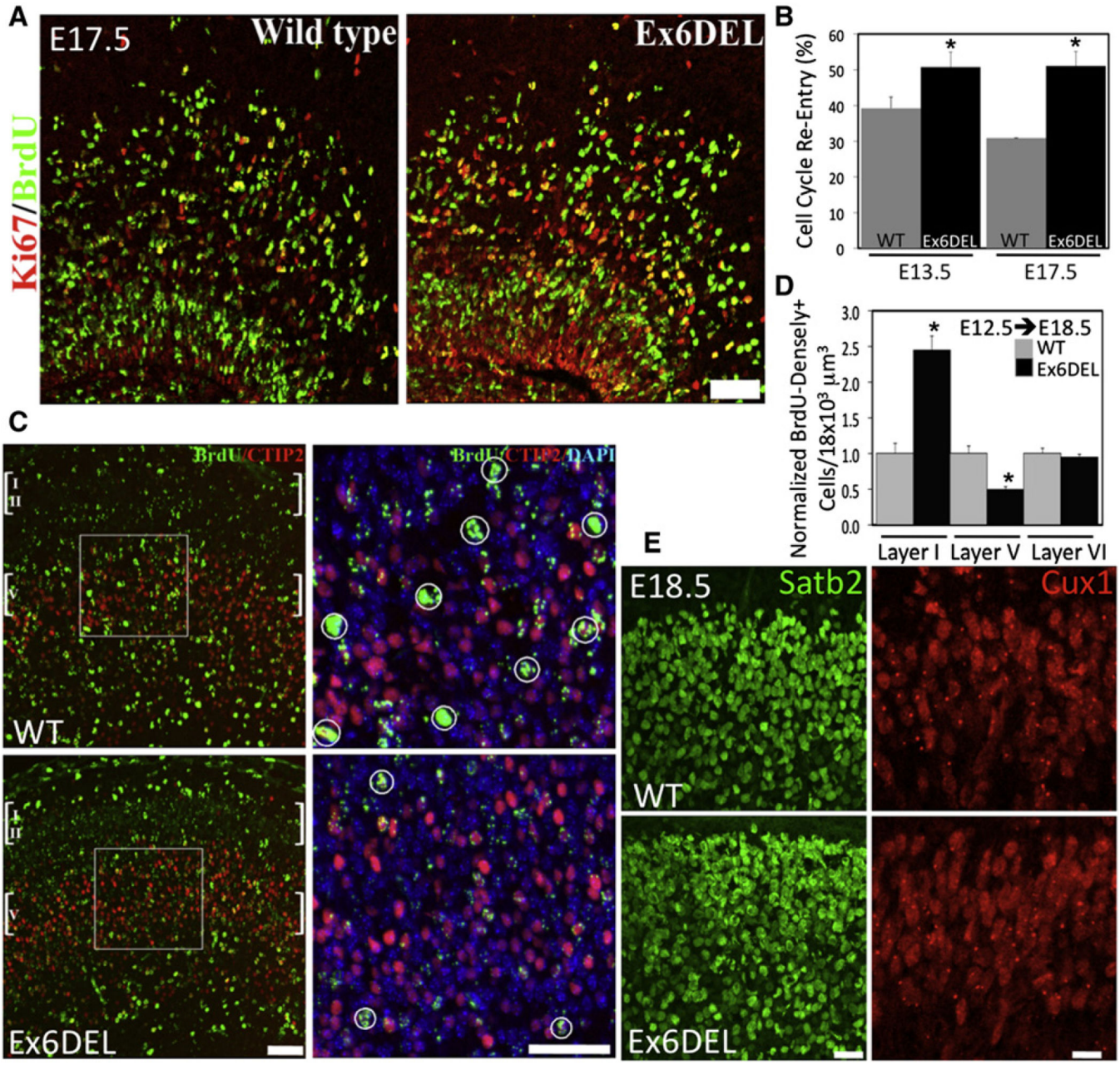

Figure 3. Delayed Neurogenesis and Increased Neuronal Output

(A) Merged images for cycling progenitors pulsed with BrdU at E16.5 then harvested at E17.5 and stained for Ki67 (red) and BrdU (green). Scale bar represents 50 µm.

(B) Plot from (A) of the percentage of cells re-entering the cell cycle ($BrdU^+$, $Ki67^+$; n = 9).

(C) E18.5 sections stained for CTIP2 and BrdU following neuronal birthdating at E12.5. Scale bar represents 50 µm. Boxed region is enlarged on right and brightly-fluorescent $BrdU^+$ cells are circled. Scale bar represents 20 µm.

(D) The location of BrdU-densely$^+$ cells from (C) were quantified and normalized to WT levels (n = 3).

(E) E18.5 sections stained for SATB2 and Cux1, markers of superficial neuronal layers. Scale bars represent 50 μm. For (B) and (D), bars represent the mean ± SEM; *p < 0.05 by t test.

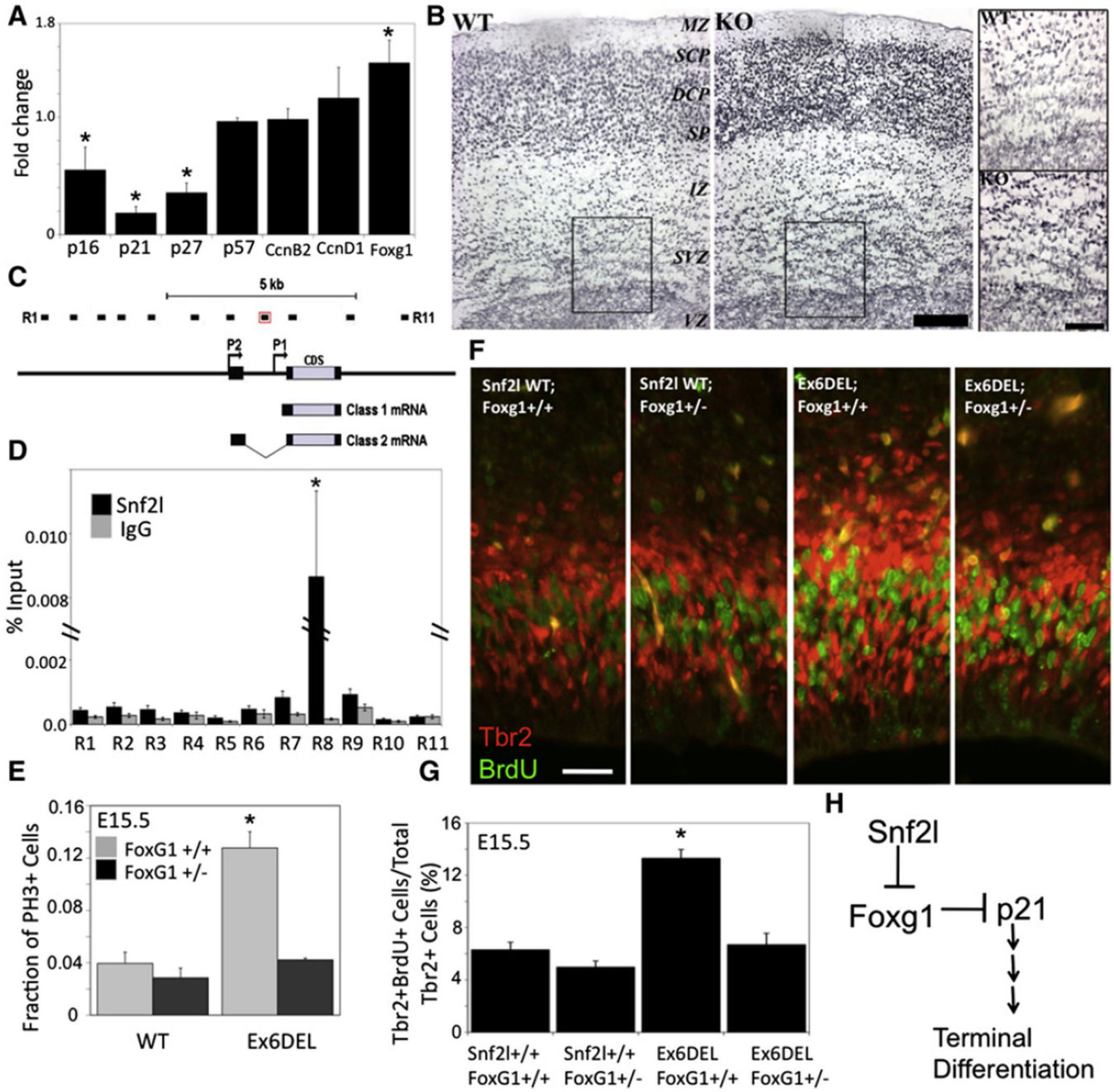

Figure 4. Foxg1 Is Misregulated in Ex6DEL Mice

(A) qRT-PCR analysis of Foxg1, cdk inhibitors (Cdnk1a, 1b,1c, 2a), and cyclins (Ccnb2, Ccnd1) normalized to WT levels (n = 3; bars represent the mean ± SEM; *p < 0.05 by t test).

(B) Foxg1 immunohistochemistry of E17.5 cortical sections. Scale bar represents 50 μm. Boxed region within SVZ is enlarged on right. Scale bar represents 20 μm.

(C) Schematic diagram of the Foxg1 locus showing the location of qPCR primer pairs R1–R11 used for ChIP analysis. P1 and P2 represent alternative promoters driving expression of class 1 and 2 Foxg1 transcripts, respectively.

(D) ChIP analysis depicting the binding of Snf2l relative to%input across the Foxg1 locus. There was a significant level of Snf2l binding over IgG control at the R8 primer set ($p < 0.012$ by t test). Each bar represents the mean ± SD from three biological replicates (each replicate represents a pool of E15.5 dissected cortices from 10 embryos) and two qPCR reactions from each replicate.

(E) Proportion of mitotic ($PH3^+$) cells in WT or Ex6DEL mice with normal ($Foxg1^{+/+}$) or reduced ($Foxg1^{+/-}$) Foxg1 dosage (n = 3; bars represent the mean ± SEM; *$p < 0.05$ by t test; PH3 stained images are shown in Figure S3G).

(F) E15.5 cortical sections from indicated genotype stained for Tbr2 (red) and BrdU (green) to identify cycling IPCs. Scale bar represents 50 μm.

(G) The proportion of Tbr2, BrdU-double labeled cells was rescued on the $Foxg1^{+/-}$ background (n = 3; bars represent the mean ± SEM; *$p < 0.05$ by t test).

(H) Model suggesting that Snf2l represses Foxg1 expression allowing for p21 derepression and the promotion of terminal differentiation.